Degradation of a Poly(ester urethane) Elastomer. IV. Sorption and Diffusion of Water in PBX 9501 and its Components

Michael R. Salazar,[1]* Shelley L. Thompson,[2] Kenneth E. Laintz,[2] Thomas O. Meyer,[3] Russell T. Pack[1]

[1]*Theoretical Division (T-12, MS B268), Los Alamos National Laboratory, Los Alamos, New Mexico 87545*
[2]*DX Division (DX-2, MS C920), Los Alamos National Laboratory, Los Alamos, New Mexico 87545*
[3]*BWXT Pantex, LLC (Mail Drop 11-2), P. O. Box 30020, Amarillo, Texas 79120-0020*

Received 5 September 2006; accepted 4 January 2007
DOI 10.1002/app.26207
Published online 9 April 2007 in Wiley InterScience (www.interscience.wiley.com).

ABSTRACT: In preparation for studying the hydrolytic degradation of Estane® 5703 in the plastic-bonded explosive PBX 9501, the sorption (solubility) and diffusion of water in PBX 9501 and each of its components are studied experimentally and modeled theoretically. Experiments are reported that measure the weight gain or loss due to a change in the relative humidity (RH). For all of the components, the equilibrium amount of water sorbed per gram of sample is linear in the RH at low relative humidities but curves upwards at higher relative humidities. This behavior is modeled with a water cluster model. Diffusion coefficients are determined by modeling the time dependence of the water concentrations assuming Fickian diffusion, and that fits the data for some of the materials. However, all the samples that contain the explosive HMX show much more complicated behavior at high relative humidities, and that is presented and discussed. © 2007 Wiley Periodicals, Inc.† J Appl Polym Sci 105: 1063–1076, 2007

Key words: degradation; diffusion; hydrolysis; polyurethanes; solubility

INTRODUCTION

The Plastic-bonded explosive PBX 9501 is widely used in weapons. It is nominally 94.9% HMX, 2.5% Estane® 5703, 2.5% nitroplasticizer (NP), and 0.1% of an antioxidant stabilizer (usually diphenylamine or Irganox 1010) by weight.[1] The HMX (1,3,5,7-tetranitro-1,3,5,7-tetraazacyclooctane) is the high explosive. The Estane 5703 (herein usually simply called Estane) is a commercial thermoplastic poly(ester urethane) polymer that was formerly manufactured by BF Goodrich[2] and is now manufactured by Noveon. The Estane is a multiblock copolymer; its urethane blocks tend to collect together to form hard segment domains that give the polymer its strength. The ester blocks (soft segments) give the polymer its flexibility. The NP is a eutectic mixture of bis(2,2-dinitropropyl) acetal (BDNPA) and bis(2,2-dinitropropyl) formal (BDNPF) and is a liquid at atmospheric pressure and room temperature.[3] In PBX 9501 the HMX is present as micron-sized particles, and the Estane, NP, and stabilizer form a binder layer that coats the HMX particles, glues them together, and decreases the mechanical sensitivity of the explosive, so that it can be molded, machined, and handled safely.

The Estane in PBX 9501 slowly degrades in storage, and that is of concern because it can alter the mechanical properties of the explosive. Our objective in this series of papers is to understand this degradation and be able to model it in detail for all likely storage conditions. One of the main mechanisms of Estane degradation is hydrolysis, and that was studied in detail in the earlier papers in this series.[4–6] It was shown there that hydrolysis is able to account for all the observed molecular weight loss for Estane 5703 degradation in indoor storage at ambient temperatures and humidities. Since water is one of the reactants in hydrolytic degradation, it is desirable, as part of this study, to know how much water is present in the PBX, where it resides, and how readily it can diffuse into or out of the PBX and its components.

PBX 9501 is formulated wet. The HMX particles are suspended in water, and the binder materials (Estane, NP, and stabilizer) are dissolved in an organic solvent. When this binder lacquer is added to the HMX/water suspension, it coats and agglomerates the HMX

Correspondence to: R. T. Pack (rtpack@lanl.gov).
**Present address*: Department of Chemistry, Union University, 1050 Union University Drive, Jackson, Tennessee 38305.

Journal of Applied Polymer Science, Vol. 105, 1063–1076 (2007)

particles. Water can be trapped at this time. Filtration and drying then produce PBX 9501 molding powder, which is stored until needed and then pressed into any shape desired. Final shaping is done by wet machining, so that the PBX 9501 can again sorb water.

The absorption and diffusion of water in neat Estane 5703 and related polymers were studied in the first paper[4] in this series. However, until now, little has been known about the moisture properties of the other components of PBX 9501. Because of its polar nitro and ether groups, the NP is expected to form hydrogen bonds with water and thus absorb it. Furthermore, the NP can undergo hydrolysis at the ether link to form 2,2-dinitropropanol, formaldehyde, and acetaldehyde.[7] The alcohol produced, 2,2-dinitropropanol, is acidic, and that is a concern because the hydrolysis of Estane is acid catalyzed. Regarding the HMX, it is commonly stored in water, and it is often thought that HMX is not even wet by water. However, one earlier study[8,9] found that HMX would sorb water at high relative humidity (RH), and the results of the present work confirm that.

In the present article we report experiments and models for the sorption and diffusion of water in all the major components of PBX 9501 both as separate components and as combinations. In the next section, the experiments and their uncertainties are described. The Sorption Results and Calculations section describes the modeling calculations and results, first for sorption. Then, the Diffusion Results and Calculations section describes the results and modeling calculations for diffusion. After that, in the Discussion section, we discuss and attempt to understand the results, and the final section contains our conclusions.

EXPERIMENTAL

LANL experiments

The Estane used in the experiments performed at Los Alamos National Laboratory (LANL) has been described earlier.[4–6] The NP used was taken from a large lot (Lot AF-OC-XB9/8) of NP that is stored at the Pantex plant in Amarillo, TX. It is tested periodically and is staying within specifications. It contains about 0.1% of phenyl-β-naphthylamine (PBNA, aka Neozone D) as a stabilizer. The binder (Estane, NP, and Irganox stabilizer in a 1 : 1 : 0.04 mixture by weight) used in these experiments was formulated at LANL. The components were dissolved in methylethyl ketone (MEK) and then poured out and dried. Upon being placed in a vacuum hood to evaporate the MEK solvent, the binder soon became solid, but it was kept in the hood for several months to remove the last of the MEK and stabilize its weight. It is in the form of sheets $\sim$ 0.6 cm thick.

Experiments were also performed on neat HMX. The HMX used was from Lot HOL-83B03-044C, which was synthesized at Holston Army Ammunitions plant in Kingsport, TN. It consists of a powder composed of micron-sized crystals mixed in a 3/4 coarse and 1/4 fine particle size combination by weight. The Mil Spec of the coarse powder is Class 1 Grade B with a mean particle size of 200 μm, and that of the fine powder is Class 2 Grade B with a mean particle size of 5 μm. Experiments were performed on the powder with the mixed particle sizes, on powder containing only the coarse particles, and on half inch by half inch cylinders made by pressing the mixed powder. The mixed powder has a bulk density of 1.234 g/cc; the coarse powder has a bulk density of 1.258 g/cc; the pressed cylinders have an average density of 1.870 g/cc; and the theoretical maximum density of HMX is 1.905 g/cc.[10]

Samples of PBX 9501 molding powder were also used in these moisture studies. The PBX 9501 molding powder used at LANL was from Lot Number 7278, which was formulated at LANL in March 1999, and from Lot 730-010, which was formulated at Holston Army Ammunitions plant in April 1989. The molding powder prills vary widely in size and shape. For example, for lot 730-010, the average diameter of the prills or particles was 0.235 cm, but the standard deviation of that diameter was 0.134 cm.[11,12] The average density of the prills themselves is 1.69 g/cc.[13]

Experiments were also performed at LANL on PBX 9501 that had been pressed into billets of average density 1.83 g/cc. Cylinders were then core machined out of these pressed billets. For brevity, these are called ''machined'' cylinders herein. These cylinders had a diameter and a length of [1/2] inch; their average mass was 2.93 g; and their average density was 1.828 g/cc. The machined PBX 9501 used at LANL was from Lot Number 730-010. Some experiments were also performed on cylinders of the same size of PBX 9501 from Lot 7278, but these were formed by directly pressing the molding powder to final size and are called ''pressed'' cylinders herein. Their average mass was 2.94 g, and their average density was 1.838 g/cc.

As explained in more detail in Ref. 4, five RH chambers were used. The first, which contained DRIERITE® desiccant, was well sealed and expected to maintain a room temperature RH of 0.02%, which differs negligibly from zero for our purposes. Three more chambers were controlled by using saturated salt solutions,[4] were well sealed, and maintained RHs of 23, 76, and 95%. (A few additional experiments were performed with the 23% chamber replaced by a chamber controlled by a saturated solution of LiCl and expected to have a RH of 16%). The fifth and last chamber was controlled by saturated potassium

carbonate solutions, but it contained the balance, could not be sealed as well, and was also disturbed whenever the door was opened to add or remove samples or change the data recording frequency. Its RH would nominally be expected[4] to be 43%, but the drier atmosphere of the laboratory caused its RH to more often be 40–42%. However, when new solutions were first made up, the RH of this chamber was higher than that, and one set of experiments herein was performed when its RH was 55%. Hence, for the balance chamber, the reading of a hygrometer probe, rather than the literature value of the RH, was used. In all the chambers, the RH was monitored, as described in Ref. 4, to within an accuracy of ±2% at the mid-range of RHs (~ 50%) and ±4% on the extremes.

As described in Ref. 4, sorption and diffusion data were obtained by placing a sample of each material in one of the chambers, at a constant RH of 0, 23, 76, or 95% for a time thought long enough for it to come into equilibrium. (Unfortunately, the time each sample was in a given chamber was not recorded.) Then, the sample was transferred to the balance (Ohaus Explorer Analytical Balance) in the 42% RH chamber, and its mass as a function of time was recorded by a TAL technologies software wedge. The mass measurements were initially recorded at time intervals of 10 s. When the experiments had gained or lost most of the water, the time interval was changed to one minute and then finally to 10 min. In practice,[4] for this long-time weighing, the accuracy of the balance is usually observed to be ±0.2 mg, with occasional time-dependent excursions (perhaps caused by power fluctuations) that are as large as ±1.0 mg.

The above paragraphs describe most of the LANL experiments reported herein. However, in a few of the later experiments, the salt solutions were used to hold the balance chamber at about 94% RH, and samples were equilibrated at low RH and then transferred to the balance chamber. Also, in one last experiment, one sample was left of the pan of the balance, and the salt solutions were changed repeatedly to cycle the balance chamber between 25 and 94% RH.

In the earlier experiments reported herein (performed between mid 1999 and mid 2001), the materials were taken in ''as received'' condition and put into the various RH chambers. However, with those materials, slow, long-term weight losses were often observed. These seem to be due to a slow outgassing of solvents, such as MEK and isopropyl alcohol (which are used in the manufacture and storage of the materials), the evaporation of NP, etc. After mid 2001, all samples were desiccated in a vacuum oven at 60°C overnight and then placed in a desiccator jar containing DRIERITE® for a minimum of 1 day before use. That decreased the slow losses markedly.

One major source of error in these experiments is due to fluctuations in the barometric pressure which causes fluctuations in the buoyancy of the air and the apparent masses of the samples. The barometric pressure was not monitored in these experiments. Another source of error is fluctuations in the RH of the balance chamber whenever its door is opened. Another source of error is any variation in the temperature. This can cause the equilibrium amount of water absorbed by the sample to change and also cause the water vapor pressure due to the salt solutions to change.

The average temperature during the experiments was 21.5°C. For some of the first measurements made, the air conditioning in the laboratory was not functioning properly, and the temperature sometimes varied by ±5°C during a given 24 h period. Later, that was corrected, and the temperature was stable to within ±1.0°C.

To get mass changes large enough to measure reasonably stably, the sample sizes used in this experiment were ~ 50 g for the NP measurements, ~ 12 g for the binder measurements, ~ 120 g for the neat HMX measurements, ~ 117 g (40 cylinders) for the machined PBX 9501 measurements, and ~ 29.4 g (10 cylinders) for the pressed PBX 9501 experiments. As will be seen later in this paper, this last sample was almost too small.

PX experiments

These experiments were performed at the Pantex (PX) plant in Amarillo, Texas, and they all used PBX 9501 from Lot 730-010, which was purchased new from the Holston Army Ammunitions plant on April 10, 1989. Since its purchase, Lot 730-010 has been stored in molding powder form in bunkers at the Pantex plant. For these experiments the molding powder was pressed into billets on November 25, 1998, and these billets had an average density of 1.829 g/cc. Cylinders, which had a diameter and a length of 1 in., weighed an average of 24.1 g each and had an average density of 1.822 g/cc, were core machined from these billets in early June of 1999. These cylinders were then stored in sealed bags at ambient conditions until September 1, 1999, when they were placed in a desiccator and allowed to equilibrate until these experiments were started on August 3, 2000.

In these experiments the cylinders were transferred from the desiccator to chambers whose temperature was (22 ± 1)°C and whose RH was controlled by 400 mL beakers of saturated salt solutions. The salts used were lithium chloride and calcium chloride, and the beakers in one chamber simply contained

distilled water. The average RH maintained in each of the chambers (including the desiccator) is estimated to be 5, 22, 34, and 95%. These were monitored using inexpensive ''Digital Relative Humidity/Temperature Meter with Minimum/Maximum Memory'' probes made in China by Control Company. Each device has calibration traceable to NIST (National Institute for Standards and Technology) with a specification hygrometer range of 25–95% and stated accuracy of ±2% in mid-range and ±4% at ends of range. Because the lithium chloride controlled RH was not in the calibrated range, all eight Control Company units available were compared with an Omega RH411 hygrometer (calibration traceable to NIST over a range of 5–99% RH). All eight units indicated either 19 or 20% after 24 h in a closed office cabinet with the RH411 probe while the RH411 m indicated 19% RH in the space. This was better performance than expected. Consequently, their readings (~ 22% RH) were used for the chambers controlled by the LiCl solutions rather than literature values.

Each cylinder was weighed as it was transferred from the desiccator to one of the chambers. Then, to follow its mass in time, each cylinder was periodically removed briefly (for 3–4 min) from its chamber and weighed and then returned to its chamber. It was found from preliminary experiments that measuring the masses daily disturbed the RH in the chambers enough and had the cylinders out in the drier atmosphere of the laboratory long enough to slow their weight gain. Hence, the masses were measured after 1 day in the chamber and then only weekly after that. The balance used to measure the masses was a Mettler Toledo Model AG245.

In addition to the cylinders, some of these same experiments were also performed on some samples of PBX 9501 prepared for use in tensile tests. These samples are in a ''dog bone'' shape; they are described in more detail later in the paper.

SORPTION RESULTS AND CALCULATIONS

Absorption of water by the NP and binder

In the LANL experiments, the amount of water gained or lost by the samples of each material, in going from one of the (0, 23, 76, or 95% RH) chambers to equilibrium in the balance at ~ 40% RH, was measured. The masses lost or gained in each experiment were added to or subtracted from the mass gained in the 0–40% RH experiment to obtain the amount of water the samples contained at equilibrium at their initial RH. Figure 1 is a plot of the experimental data for the absorption of water (in milligrams of water absorbed per gram of sample) by the nitroplasiticizer (NP) (triangles) and binder (diamonds) as a function of the RH. The multiple measurements at 40% RH were obtained by desiccating samples after they had established equilibrium with the 40% RH environment and measuring the mass lost. The error bars along the x-axis reflect the uncertainty (estimated to be ±2%) in the RH due to the saturated salt solutions and hygrometers, while the errors along the y-axis reflect the uncertainty (estimated to be ±0.25 mg/g) in the weight measurements.

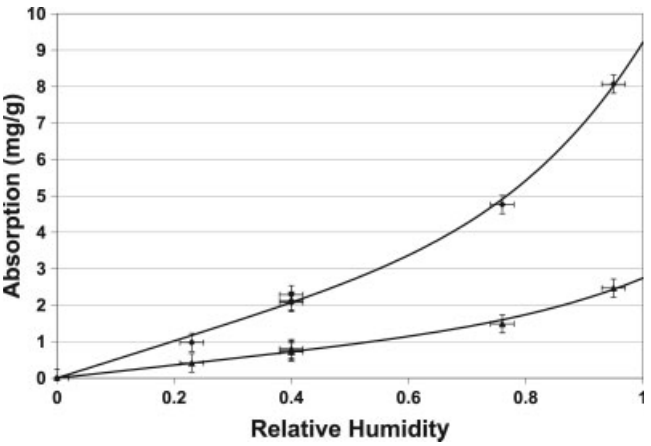

Figure 1 Absorption (mg water per g material) of water versus RH as a fraction. Diamonds-binder; triangles-NP. The points are experimental; the lines are the fit of the cluster model.

From Figure 1 it is evident that the absorption of water by the binder is a Type III isotherm[14]; i.e. it is linear in the RH at the lower RHs (<~50%) but curves upward at higher RHs. This behavior was also observed in neat Estane.[4] The absorption profile for the neat NP is more nearly linear than that of the binder but also curves upward somewhat at high RH. At 50% RH, the sorption or solubility (S) of water in the binder and NP are estimated to be 2.7 and 0.9 mg of water/g of sample, respectively, as shown in Table I. We note that, at this RH, the water absorbed by neat Estane is about 6 mg/g.[4]

The water cluster model discussed in Ref. 4 was used here to describe the nonlinear equilibrium absorption of water at high RHs. Briefly stated, the absorbed water is modeled to exist as either water monomers, W, or water clusters, W_n, containing n water molecules. The absorbed water monomers are in equilibrium with the water vapor in the surrounding atmosphere and also in equilibrium with water clusters in the material. The total concentration of absorbed water is the sum of contributions from the monomers and clusters. These contributions may be written in terms of the partial pressure of water in the atmosphere, the equilibrium constant (K_1) between the momomers and the vapor phase, and the

TABLE I
Experimental Results for the Sorption of Water by the Components of PBX 9501

Component	S (mg/g) at 50% RH	K_1 (atm-kg/mol)	n	K_n $(\text{kg/mol})^{n-1}$
Binder	2.7	0.0902	5	25.6223
Nitroplasticizer	0.9	0.2570	5	1.1149×10^3
Neat HMX	0.017	14.6295	10	4.1217×10^{25}
PBX 9501–all forms	0.17	1.4636	5	2.9848×10^6

equilibrium constant (K_n) between monomers and clusters as:

$$[H_2O]_{total} = p/K_1 + nK_n p^n/K_1^n, \quad (1)$$

and the nonlinear dependence on the water vapor pressure, p, is clear. In Ref. 4 it was found that the value $n = 5$, for the number of water molecules per cluster, best fit the data for Estane, and, for convenience, that same value is simply used here for NP and binder. The equilibrium constants of eq. (1) for the NP and binder are reported in Table I, and the solid lines in Figure 1 are the fit of the cluster model to the experimental data. It should be noted that the equilibrium constants reported in Table I intentionally have more significant figures than are warranted; that allows reproduction of the absorption profiles.

Sorption of water by neat HMX

The sorption of water by neat HMX was also measured as a function of RH using the method described in the preceding subsection. The results are shown in Figure 2. The squares shown are the results for the 3 : 1 mixture of coarse to fine HMX powder. The triangles are the results for coarse HMX powder, and the circles are the results for the neat HMX pressed into half inch cylinders. The error bars on each are those due to oscillations in the observed weights of the samples. However, the true uncertainties may to be considerably larger than that. It is not clear whether the differences between the samples composed of HMX in different forms are really due to the differences in form or to experimental uncertainty in such things as the RH. At high RH where the curve is steep this uncertainty could have a large effect.

One sees that HMX sorbs very little water at low relative humidities-so little that the relative uncertainties are quite large. However, it sorbs more water at high RH. This behavior, with the sharp curvature (upturn) at high RH, requires that a large n be used in the water cluster model. The fit of the 3 : 1 powder data, shown by the solid line in Figure 2, has $n = 10$, and the linear term is very small. This behavior probably does not represent a cluster of water molecules around a single hydrogen bonding site but is characteristic of a hydrophobic interaction[8,9] and is more likely to represent condensation in pores[14] where a number of sites are fairly close together. Thus, it may be better described as adsorption rather than absorption. Hence, for this system, we view the water cluster model as simply a fitting form and do not attribute much physical meaning to it. The sorption of water by HMX powder at 50% RH is estimated to be only 0.017 mg/g. Our sorption results agree qualitatively with those of Castorina and Haberman.[8,9] Quantitatively, our results lie lower than theirs at low RH and between the results for their ground and unground samples at high RH. Such differences are to be expected because this sorption is a surface effect, sensitive to differences in grinding, and our HMX was ground differently than theirs.

Sorption of water by PBX 9501

The sorption of water by samples of PBX 9501 in several forms was measured. PBX 9501 is a heterogeneous solid consisting of the micron-sized particles of HMX glued together by a film of binder. In experiments on some of the forms of PBX 9501, gain or loss of the water occurred on different time scales

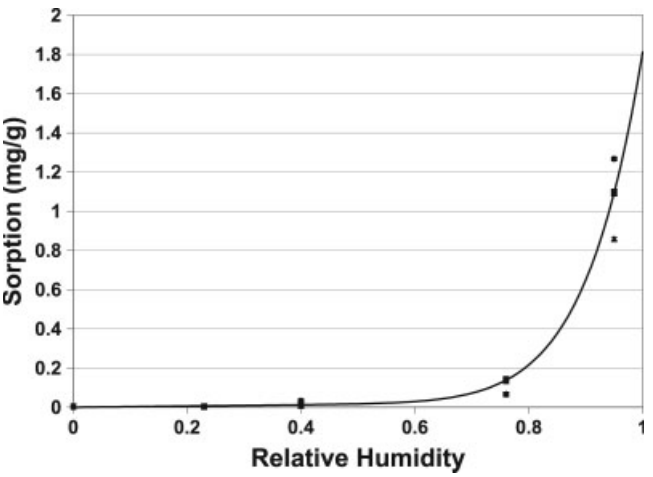

Figure 2 Sorption of water (mg/g) by neat HMX versus RH as a fraction. The points are experimental; the line is the model. Squares-sorption by 3 : 1 mixed powder; triangles-sorption by coarse powder; circles-sorption by pressed cylinders of HMX. The line is a fit to the squares.

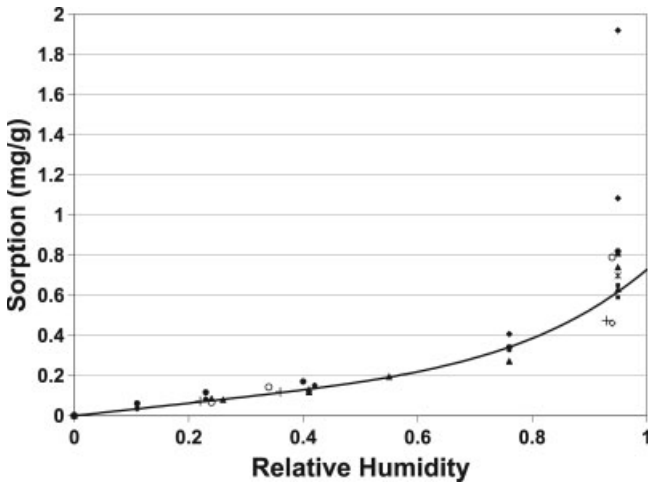

Figure 3 Sorption of water by PBX 9501 in mg/g versus RH as a fraction. The points are experimental; the line is the model. Diamonds-total sorption by the LANL machined cylinders; squares-binder contribution to sorption by the LANL machined cylinders; triangles-total sorption by the molding powder; solid circles-total sorption by the LANL pressed cylinders; asterisks-binder contribution to the sorption by the LANL pressed cylinders; open circles-total sorption by the ''dog bone'' tensile samples; plus signs-total sorption by the PX machined cylinders; open diamond-total sorption by machined cylinders in LANL 0–95% experiment. The line is a fit to the squares. It includes only the contribution due to the binder.

that allowed approximate separation of the sorption due to the HMX from that due to the binder, and that will be discussed in more detail in the Diffusion section of this paper. Here we discuss the sorption.

Molding powder

The sorption isotherm for water by PBX 9501 molding powder is shown as the triangles in Figure 3. These data are for both lots (Lot 7278 and Lot 730-010), as they differed negligibly. In the molding powder, the sorption and desorption by the HMX and binder occur on the same, rapid time scale and could not be separated, so all that is shown is the total sorption. Error bars are not shown on this plot to avoid covering other data points; the estimated error bars on each point, due to the balance, etc., are about the differences seen between all the different 40% RH samples. The sorption of water at 50% RH for the molding powder (and all other forms of PBX 9501) is estimated to be 0.17 ± 0.03 mg/g. One will note that at the higher relative humidities, the uncertainty is larger due to some irreproducibility which will be discussed later in the paper.

LANL machined cylinders

The sorption of water by the LANL [1/2] in. × [1/2] in. machined PBX 9501 cylinders is also shown in Figure 3. The estimated separate contribution to the sorption due to the binder is shown as the squares, and the total sorption is shown as the diamonds. At low RH the squares are superimposed on the diamonds because the total sorption differs negligibly from that by the binder. At high RH, one should note that there is a large variability in the total sorption; there it depends on the detailed history of the samples and will be discussed more later in the paper. The solid line is a fit of the cluster model with $n = 5$ to the binder portion of the sorption by the LANL machined cylinders. It is representative of all the forms.

LANL pressed cylinders

To see if the differences in the surfaces of cylinders that were directly pressed to final shape (without being machined) have any effect, sorption data were also obtained on pressed cylinders of PBX 9501. The data for total sorption are shown as solid circles. The sorption of the binder can only be distinguished from the total at the highest RH where it is shown as the asterisk. These data used samples of a smaller total weight than used for the machined cylinders, so that their uncertainty is greater. To within mutual uncertainties, the binder-only absorption by the pressed cylinders agrees with that of the machined cylinders.

PX machined cylinders and tensile specimens

The data for the PX experiments using 1 in. × 1 in. cylinders are shown as the plus signs in Figure 3. Each data point is the average for at least three cylinders. The sorption by these samples appears to all be due to the binder; no sorption by the HMX was observed in them. They agree within mutual uncertainties with the curve. These are all sorption experiments in which the change of mass in going from a very low RH to a higher RH was measured. The longest any of them ran was for 70 days, and, in retrospect, they may not have been fully equilibrated. Sorption experiments were also performed on tensile specimens. These are made by machining cylinders that are 3 in. long by 1 in. in diameter from pressed billets of PBX 9501. Then the cylinders are further machined into the shape of a ''dog bone'' in which the narrow part of the cylinder is [1/2] in. in diameter, but the ends are still near 1 in. in diameter. The results on these are shown as the open circles in Figure 3. They agree with all the other samples at low relative humidities. However, these samples ran as long as 294 days, and one sees that the open circle at 94% RH is higher than the curve. As will be discussed more later in the paper, we believe that this sample is beginning to show some sorption by the HMX, but we cannot separate that from the total.

DIFFUSION RESULTS AND CALCULATIONS

Diffusion of water in the components of PBX 9501

To get information about the time behavior of sorption and desorption of water from the components of PBX 9501, calculations were performed assuming Fickian diffusion, and the results were compared with the experiments. Fick's second law may be written as[15,16]

$$\frac{\partial c(\mathbf{r},t)}{\partial t} = D\nabla^2 c(\mathbf{r},t) \tag{2}$$

where $c(\mathbf{r},t)$ is the concentration at position $\mathbf{r}$ at time t and D is the diffusion coefficient. The shapes of the samples varied from a thin film of solid (binder) to cylinders (machined PBX 9501) to a thin film of liquid (NP). Equation (2) was solved for the shapes of the samples to extract a diffusion coefficient for these components. The solutions of eq. (2) are proportional to $t^{1/2}$ at early times; thus, figures that give the time evolution of the concentration of water are plotted versus $t^{1/2}$. An initial linear dependence in these plots is expected for classic Fickian diffusion. Also, at long times, Fickian diffusion gives exponential behavior, and log plots (not shown) of the uptake versus time were made to look for linearity at long times. These two tests help decide whether diffusion in a given sample is Fickian.

Because the neat HMX powder has widely varying particle sizes, the PBX 9501 molding powder has a large variation in the size and shape of its prills, and the PBX 9501 ''dog bone'' samples have a complicated shape, no attempt was made to obtain diffusion coefficients from samples of these three types.

As in Ref. 4, the experimental data were fit by solving eq. (2) for the various shapes of the samples and adjusting the diffusion coefficient D to minimize the dimensionless root mean square error given by

$$\gamma = \left[\frac{1}{N}\sum_{i=1}^{N}\frac{[c(t_i) - cx(t_i)]^2}{\Delta_i^2}\right]^{\frac{1}{2}} \tag{3}$$

where N is the number of experimental data points, c is the calculated average concentration at time t_i, cx is the experimental average concentration at time t_i, and Δ_i is the uncertainty in cx. The dimensionless root mean square error is less than (greater than) unity if the average theoretical fit is within (outside of) the experimental error limits.

Diffusion of water in the binder

The time dependence of the water concentration in the binder samples plotted versus $t^{1/2}$ is shown for the different experiments in Figure 4. Their uncertainties (not shown) are taken to be $\Delta_i = 0.25$ mg/g, consistent with the absorption data. The lines are the results of fitting the data as one-sided diffusion in a thin film with a diffusion coefficient $D = (2.5 \pm 0.5) \times 10^{-6}$ cm^2/s. The dimensionless root mean square error γ of the four experiments is 0.31, so that all four experiments are fit well within their error bars. The near linearity of the data in $t^{1/2}$ at short times in Figure 4 and the exponential behavior at long times (not shown) both indicate that the diffusion is Fickian to within experimental error. The uncertainty in the diffusion coefficient was estimated from the deviations of the best-fit D coefficients of the individual experiments from the overall best fit single D noted above. This diffusion coefficient is given in Table II along with the half-life (the time it takes for half the weight change to occur), and the time it takes to come to equilibrium (t_{eq}) at low and high relative humidities. Not all of the data taken in these experiments are shown in Figure 4. Only every 70–150th data point (depending on how many points were taken in each experiment) is shown for economy of presentation.

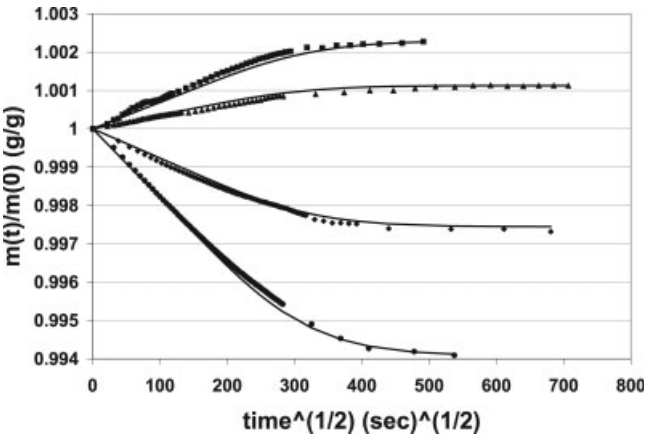

Figure 4 Mass of the binder versus the square root of time ($s^{1/2}$). The squares are for the 0 → 40% experiment; the triangles are the 23 → 40% experiment; the diamonds are the 76 → 40% experiment, and the circles are the 95 → 40% experiment. The lines are the fit by the diffusion model.

Diffusion of water in the NP

The time dependence of the water concentration in the NP is shown in Figure 5. In the experiments in which mass was gained, the mass initially has a linear dependence in the concentration versus $t^{1/2}$; however, the experiments in which water was lost have curvature due to an initially slower mass loss followed by a faster loss. Also, all four experiments show a slow and continual mass loss at long times. This long-term slow mass loss is believed to be due

TABLE II
Fickian Diffusion Coefficients, Half Lives, and Time to Equilibrium for Water in PBX 9501 and its Components

Component	D (cm^2/s)	$t_{1/2}$ (h)	t_{eq} (h) low RH	t_{eq} (h) high RH
Binder–0.6 cm thick	$(2.5 \pm 0.5) \times 10^{-6}$	8.3	100	100 for loss
Nitroplasticizer–0.7 cm thick	$(5 \pm 3) \times 10^{-6}$	7.5	70	70 for loss
Neat HMX–all forms		0.5 at low RH, 12 at high RH	1	180 for loss
PBX 9501–molding powder	$\sim 10^{-7}$	0.7	4	>70 for loss
PBX 9501–dog bones		67 low RH, 180 high RH	1400	5400 for gain
PBX 9501–1.0'' cylinders	$(1.8 \pm 0.3) \times 10^{-7}$	67 low RH, >120 high RH	1400	>1400 for gain
PBX 9501–0.5'' cylinders	$(1.8 \pm 0.5) \times 10^{-7}$	25 low RH, 4 high RH loss	350	350 for loss

to the slow evaporation of the liquid NP.[17] To account for it, the experimental data were fit by the following equation,

$$m(t) = m_{H_2O}(t) + m_{NP}(0)\, e^{-kt} \quad (4)$$

where $m_{H_2O}(t)$ is the mass of water at time t calculated from the solution of eq. (2) for one-sided diffusion in a thin film, while the second term represents the evaporation of NP. The rate coefficient, k, in the second term was obtained by first fitting only the long-time data, and an average value of k of 2.3×10^{-10} s^{-1} was obtained. Using this k, the evaporation term was subtracted from the experimental data at each time, and D was obtained by fitting with the remainder of eq. (4). The best fit D coefficients for the individual 0 → 40, 23 → 40, 76 → 40, and 95 → 40% RH experiments are 3.9×10^{-6}, 2.9×10^{-6}, 7.6×10^{-6}, and 7.1×10^{-6} cm^2/s, respectively. The resulting fits to the experimental data are the solid lines in Figure 5. Because the D coefficients for water loss are a factor of two larger than those for water gain, the average overall D reported in Table II is quite uncertain. The average value of γ for the experiments was 0.095 when a constant uncertainty of $\Delta_i = 0.25$ mg/g was used, so that using different D coefficients for the individual experiments fits them within their uncertainties, but the diffusion is clearly not really Fickian. Average values of the half-life ($t_{1/2}$) and time to equilibrium (t_{eq}) at low and high RH are listed in Table II. These results will be discussed further in the Discussion section.

Diffusion of water in neat HMX

HMX powder

The time dependence of water uptake and loss by neat HMX powder (in the 3 : 1 coarse to fine mixture) was measured and is displayed in Figure 6. Because of the wide variation in particle sizes, no attempt was made to determine any diffusion coefficient from these data, but these data can give an idea of how long a given sample might need to be dried to remove water from it. As can be seen from this figure, the amount of water sorbed in going from 0 to 40% RH was nearly the same as the amount sorbed in going from 23 to 40% RH, so that the total sorption at 23% is zero within experimental uncertainty (cf. Figure 2). Looking at the experiments in which water was lost, one sees that, from both the

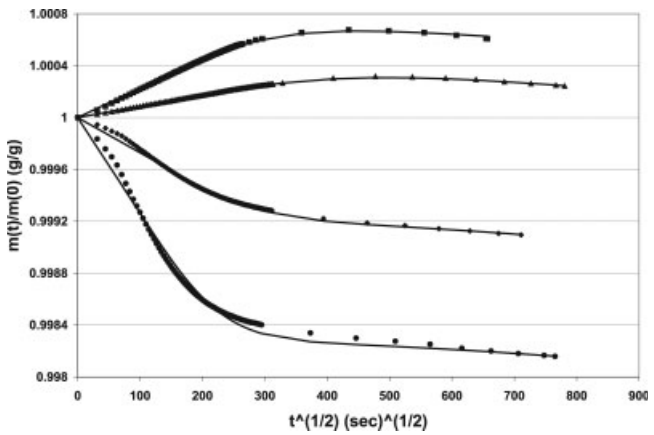

Figure 5 Mass of NP versus square root of time (s$^{1/2}$). The symbols are same as in Figure 4. See the text for discussion.

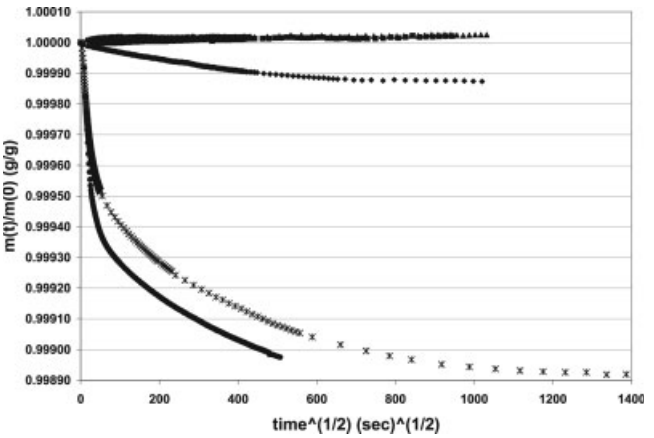

Figure 6 Mass of neat HMX 3 : 1 powder versus square root of time (s$^{1/2}$). Triangles are 0 → 40% experiment; squares are 23 → 40% experiment; diamonds are 76 → 40% experiment; circles and asterisks are repeated 95 → 40% experiments.

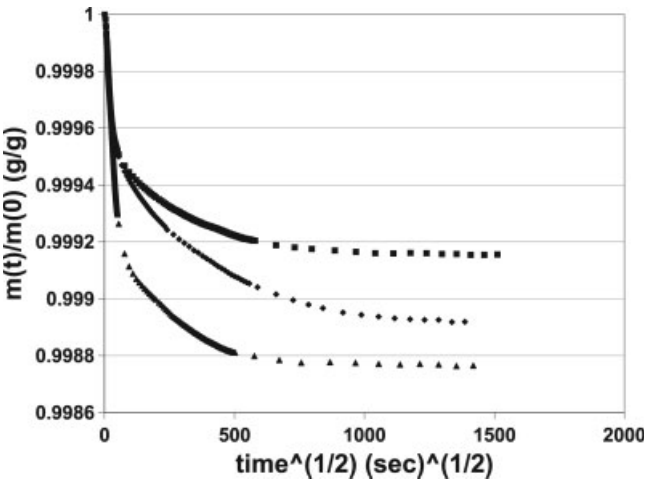

Figure 7 Mass of neat HMX versus square root of time ($s^{1/2}$) for three 95 → 40% experiments. The diamonds are for 3 : 1 coarse to fine mixed powder; the squares are for the coarse powder; and the triangles are pressed cylinders of neat HMX.

short time and the long time behavior, the process being observed is not Fickian diffusion. For example, the 95% → 40% RH experiment shows an initial rapid loss of mass (for $t^{1/2}$ up to 50 $s^{1/2}$), followed by a slower loss (for $t^{1/2}$ from 50 to 800 $s^{1/2}$), followed by a very slow loss (for $t^{1/2}$ from 800 to 1400 $s^{1/2}$). This trimodal behavior suggests that water is being lost from different binding sites on the surface of or within the HMX particles, and that will be discussed further in the Discussion section. An approximate half-life is given in Table II. Also, we note that the times to equilibrium at low and high RH reported in Table II are very different.

These experiments have also been performed on samples of HMX in other forms. The results of three 95% → 40% experiments are compared in Figure 7. The three are the 3 : 1 coarse to fine mixed powder, the coarse powder; and the neat HMX pressed into half inch cylinders. One sees that the coarse powder and the cylinders do not show the very slow loss seen in the mixed powder but become virtually flat after $t^{1/2} > 800$ $s^{1/2}$. Also, the amount of water lost from the three forms is seen to vary significantly. These features will be discussed further in the Discussion section.

Diffusion of water in PBX 9501 molding powder

The time dependence of the water uptake and loss by the PBX 9501 molding powder is shown in Figure 8. No attempt was made to model these data because of the wide distribution of sizes and shapes of the molding powder prills. The time scales are all very similar for the 0 → 42, 23 → 42, and 76 → 42% RH experiments, and they all come to equilibrium quite rapidly. The half-life and times to equilibrium at low and high RH are given in Table II. However, some of the 95 → 42% RH experiments show an additional very slow loss, and the mass lost in repeated 95 → 42% RH experiments is seen to vary. These observations will be discussed more later in the paper.

Diffusion of water in machined PBX 9501 cylinders

Pantex cylinders

The time dependence of the water concentration in the Pantex experiments with the 1 in. × 1 in. machined PBX 9501 cylinders is shown in Figure 9. Each point is the average value for three cylinders. (The values for the three cylinders differ by only a few percent from each other.) The behavior appears to be simply Fickian. Fitting all the experiments with a single diffusion coefficient gives $D = (1.8 \pm 0.3) \times 10^{-7}$ cm^2/s and the solid lines in Figure 9. The uncertainty in D was estimated from the differences between the average diffusion coefficent and the best fit values from the individual experiments. Using an uncertainty in the mass measurements of ±0.01 mg/g and the average D listed above, one obtains a dimensionless root mean square error of 0.83. These experiments seem to be coming toward equilibrium; however, none of them were run for longer than 70 days. D, the half-life, and the time to equilibrium at the lower relative humidities are all given in Table II. However, no t_{eq} for high RH is given as the sample may never really have come to equilibrium.

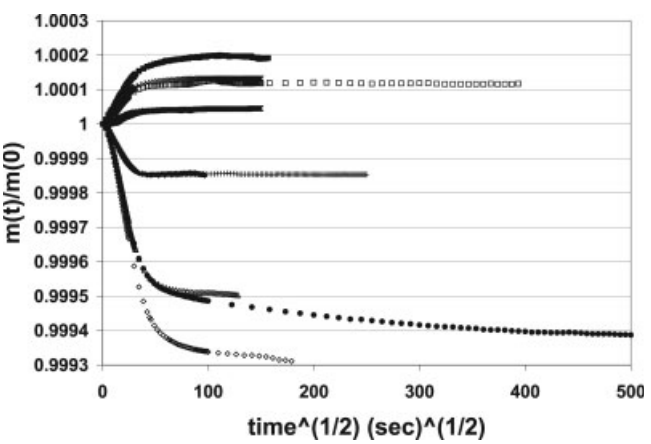

Figure 8 Mass of PBX 9501 molding powder versus square root of time ($s^{1/2}$). Starting from the top of the figure, the solid squares are 0 →55% experiment; the crosses and open squares are repeated 0 → 42% experiments; the asterisks superimposed on solid triangles are repeated 23 → 42% experiments; the solid diamonds superimposed on plus signs are repeated 76 → 42% experiments; and the open triangles, solid circles, and open diamonds are repeated 95 → 42% experiments.

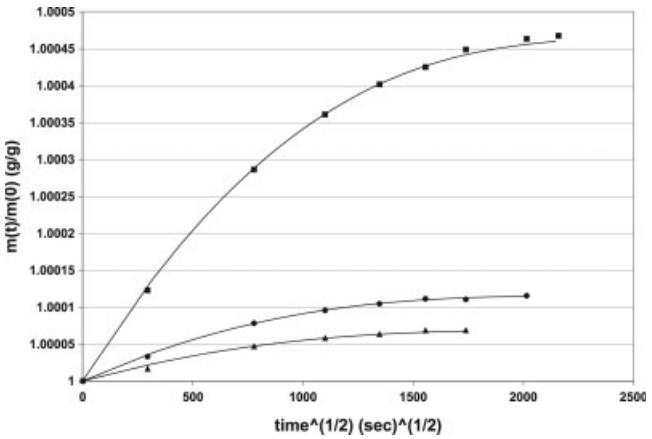

Figure 9 Mass of 1 in. × 1 in. PBX 9501 machined cylinders versus square root of time ($s^{1/2}$). Squares are 0 → 93% RH experiment; circles are 0 → 36% experiment; and triangles are 0 → 22% experiment. The lines are the fit of the diffusion model.

Pantex tensile samples

The time dependence of the sorption of the tensile (''dog bone'') samples described in the section on sorption was also measured but is not shown to save space; their weights were followed for 294 days. The samples at the lower RHs came to equilibrium within 2 months. However, the weight of the tensile samples exposed to 95% RH rose at early times, flattened out considerably near 2 months (~2000 $s^{1/2}$), and then rose again slowly and did not become constant until about 8 months had elapsed. See also Table II. We believe that the early time sorption in both the PX cylinders and tensile samples is due to the binder. The later time sorption in the tensile samples at high RH appears due to the HMX. This will be discussed further in the Discussion section.

LANL cylinders

The time dependence of the mass in the LANL experiments on [1/2] in. × [1/2] in. machined PBX 9501 cylinders is shown in Figure 10 and Table II. The 0 → 95, 0→ 42, and 23→ 42% water gain experiments appeared simple, so they were modeled using eq. (2), and a diffusion coefficient was extracted. The best fit D is the same as the D obtained from the PX 1 in. × 1 in. cylinder experiments; namely, $(1.8 \pm 0.5)\times10^{-7}$ cm^2/s, with a little larger uncertainty. The resulting fits are the lines in Figure 10 going through the 0 → 95, 0 → 42, and 23 → 42% RH data. The dimensionless root mean square errors for these experiments, using an uncertainty in the mass measurements of ± 0.06 mg/g, were 0.269, 0.049, and 0.081, respectively.

The experiments in Figure 10 that go from high to moderate RH all show a bimodal time behavior. The two 76 to 42% RH experiments (diamonds and plus signs), which are indistinguishable from each other on the scale of Figure 10, both show some rapid loss at early times followed by a slower loss. The one 95 to 42% RH experiment shown as the asterisks in Figure 10 shows a fast loss and a slow loss that are fully consistent with the 76–42% RH experiments. However, the second 95–42% RH experiment (circles) showed trimodal behavior: a moderate rate then a fast rate then a slow rate. It also lost much more mass in the fast regime than did the asterisk experiment.

To help in understanding these results, all of these water loss experiments were fit to a two diffusion coefficient model. PBX 9501 is an inhomogeneous solid, and it was assumed that the water lost in the fast and slow processes comes from different locations or sites in the solid. The total water concentration $c(\mathbf{r},t)$ was thus written as the sum, $c(\mathbf{r},t) = c_{fast}(\mathbf{r},t) + c_{slow}(\mathbf{r},t)$, and each of these concentrations was assumed to satisfy eq. (2) with its own diffusion coefficient, D_{fast} or D_{slow}, respectively. The two 76 to 42% RH experiments and the 95 → 42% RH experiment shown as the asterisks in Figure 10 were fit to determine the two diffusion coefficients. The best fit diffusion coefficients are $D_{fast} = 4.0 \times 10^{-5}$ cm^2/s and $D_{slow} = 1.8 \times 10^{-7}$ cm^2/s. The dimensionless root mean square errors (γ) obtained for these experiments are 0.074, 0.079, and 0.18 for the data represented by the diamonds, plus signs, and asterisks, respectively. Thus, these three experiments are fit well within experimental error. Regarding the experiment denoted by the solid circles, a calculation using the same two D coefficients is also shown in

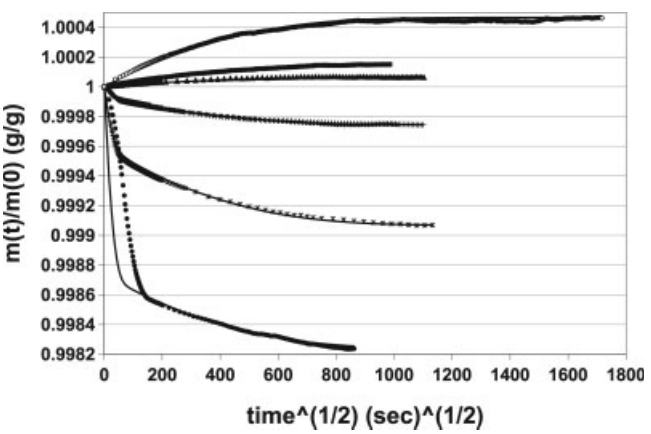

Figure 10 Mass of [1/2] in. × [1/2] in.; PBX 9501 machined cylinders versus square root of time ($s^{1/2}$). Open circles are 0 → 95% experiment; squares are 0 → 42% experiment; triangles are 23 → 42% experiment; diamonds and plus signs are repeated 76 → 42% experiments; and the asterisks and circles are repeated 95 → 42% experiments. The lines are the fits using a two diffusion coefficient model. See text for discussion.

Figure 10. Because the model is bimodal and not trimodal, it does not contain the initial moderate rate, and its γ is thus quite large, 1.7. However, because its fast loss parallels the fast experimental loss, and its slow loss parallels the slow experimental loss, it is clear that those parts represent the same processes as the fast and slow losses in the other experiments. We note, too, that the D_{slow} obtained in these experiments is the same as the D for all the PX cylinder gain experiments in Figure 9 and the LANL gain experiments in Figure 10.

The slow process observed here gives curves that behave in a way that is at least approximately Fickian. Thus, to separate the slow losses from the fast losses, linear extrapolations of the slow curves in Figure 10 to $t^{1/2} = 0$ were performed. They allow the amount of water sorbed by the binder (A_{slow} or A_{bind}) to be calculated for each experiment as well as the total sorption as shown in Figure 3. We note that sorption by the binder is quite reproducible; however, sorption by the HMX varies greatly in repeated experiments and will be discussed later in the paper. The time to equilibrium is shown in Table II, but the half-life varies widely for different experiments and different relative humidities.

Diffusion of water in pressed PBX 9501 cylinders

A few experiments were performed on half inch cylinders of PBX 9501 that were simply pressed into final shape without machining. Because the sample size was much smaller than for the machined cylinders, the results (not shown) were, as expected, much noisier. However, they displayed the same kinds of behavior as the machined cylinders, and they were modeled using the same diffusion coefficients as the data in Figure 10. The conclusions are the same as for the machined cylinders with one exception: In the mass loss experiments these pressed cylinders lost much less mass in the rapid loss mode than did the machined cylinders. In the results, one could see **no** rapid loss in the 76–42% RH experiments, and the amount of mass lost in the 96–42% experiment was much smaller than that lost in either of the corresponding experiments with machined cylinders. Whether this difference is due to the differences between the surfaces of the pressed and machined cylinders, nonequilibration at the high RH, or some other irreproducibility is not clear.

DISCUSSION

Water absorption in non-HMX containing materials

The absorption results for the binder and the NP appear to be straightforward. If the binder, which is mostly a mixture of Estane and NP, were an ideal solution, one would expect that its absorption of water would simply be the average of the absorption found here for NP and the absorption we found earlier[4] for Estane. Actually, it is slightly less than that average which indicates that the NP and Estane hydrogen bond enough with each other to use up a few of their available hydrogen bonding sites. The fact that the NP absorption isotherm in Figure 1 shows less curvature than the isotherms for binder and Estane may imply that liquid NP has fewer sites for formation of water clusters.

Water sorption by HMX-containing materials

HMX powder

The shape of the curve in Figure 2 for sorption by HMX powder indicates that, as concluded by earlier workers,[8,9] HMX is hydrophobic.[14] The rapid upturn at high RH is not from sorption of individual water molecules but is a high-order process, and both the shape of this curve and the time dependence of water gain and loss from HMX powder imply that sorption is due to condensation of water in pores or surface imperfections in the crystals. However, the fact (see Figures 6 and 7) that there is some slower (50–800 $s^{1/2}$) loss from these tiny HMX crystals suggests that there may be some absorption into the crystals themselves. Our samples of powdered HMX are supposed to be all β phase crystals. However, it is possible that, in the repeated cycling of this material between low and high relative humidities, a small amount of γ-phase HMX was formed. Castorina and Haberman[9] concluded that water sorbs into the crystals of γ-phase HMX. Later, an X-ray study[18] of γ-HMX found water in it and concluded that the γ phase is a hydrate. However, the γ phase can be prepared without using water, and a more recent study[19] of the water lost when the γ phase is heated and converted into a different phase saw no evidence of water loss. It seems likely to us that, rather than actually being a hydrate, the γ phase simply has space enough in its crystal structure to accommodate some water. It is known[9] that the γ phase loses water very slowly, and that might possibly account for the slower (50–800 $s^{1/2}$) loss seen in Figure 6.

PBX 9501

From Figure 3 one can see that, at low and moderate relative humidities, the water sorbed by the different forms of PBX 9501 differs by less than the uncertainty in the data, so that whether the material is in the form of molding powder, machined cylinders, or pressed cylinders makes no significant difference. That means that neither the surface area of the PBX nor any microcracks produced in pressing and machining make appreciable difference in the amount

of water sorbed. That is because, at the low and moderate RHs, absorption by the binder dominates the total sorption of water by PBX 9501. However, at high relative humidities, there is additional sorption due to the HMX; under the circumstances of our experiments, the amount of water sorbed by the HMX is highly variable and not reproducible. We believe that this is evidence that it has not always reached equilibrium, and it may also be due to the sensitivity in this region to the uncertainty in the measurement and stability of the RH. It may also depend on the form and history of each sample of PBX 9501. This will be discussed further in just Diffusion of Water in HMX Containing Materials subsection.

Diffusion of water in non-HMX containing materials

To within experimental error, the diffusion of water in the binder is Fickian at both short and long times. The short time behavior is shown in Figure 4; the exponential behavior at long times is not plotted but is implied by the good fit of the Fickian lines plotted in Figure 4.

The diffusion of water in liquid NP, as shown in Figure 5, shows non-Fickian behavior at short times. We expect that this is due to setting up a boundary layer on the surface of the liquid.[17] Such a layer could also explain why the apparent diffusion coefficients for uptake and loss experiments are so different; such behavior could be modeled, but it is beyond the scope of this study.

From Table II one sees that the diffusion coefficients for water in the binder and the NP are roughly the same size (10^{-6} cm^2/s), and both are an order of magnitude larger than the diffusion coefficient[4] for water in Estane 5703. Thus, the plasticization of the Estane by the NP also makes it easier for water to diffuse through it. Since diffusion through a solid is an activated process, this suggests that the water bonding sites in the binder have a different environment around them than in neat Estane. The water is probably still located around the hydrogen bonding sites of the Estane soft segment, but the presence of the NP must decrease the activation energy required for a water molecule to move from one site to another.

Diffusion of water in HMX-containing materials

Neat HMX

Figure 6 shows the time dependence of the gain and loss of water from the 3 : 1 mixed HMX powder. Although it is not clear on the scale of the plot, the 0 → 40 and 23 → 40% experiments come to equilibrium quite rapidly, typically on a time scale of 45 min (i.e. $t^{1/2} = 50$ $s^{1/2}$) or less. That also happens to be the time scale on which we estimate that water that is in the spaces between the micron-sized HMX crystals could diffuse through these spaces between the particles and get into or out of the zero to three-quarters inch deep conical pile of HMX powder which is on the weighing pan in this experiment. Hence, we cannot say whether it represents the time for water to diffuse through the HMX particles or the time for it to get into or out of the pile of HMX powder. The 95 → 40% HMX experiments show some of this same rapid loss; however, they also show a slower process during the period when $t^{1/2}$ is between 50 and 800 $s^{1/2}$. The only processes with micron-sized particles that we know of that could take that long must involve diffusing from one site to another inside the crystal lattice as was suggested in the second subsection of this Discussion section.

With regard to the very slow (800–1400 $s^{1/2}$) weight loss seen in the long low curve in Figure 6, which is also the middle curve in Figure 7, we believe that this is due to the slow outgassing of solvents used in the production of the HMX; i.e., we believe that this sample had not been baked out *in vacuo* long enough. The reason for this belief is that the other two samples shown in Figure 7 do not show this very slow weight loss even though one is a powder similar to the first sample, and the other is a cylinder made from the same 3 : 1 powder as was used in the first sample.

PBX 9501 molding powder

The time dependence for the PBX 9501 molding powder is shown in Figure 8. Most of the experiments come quickly and smoothly to equilibrium in $\sim$ 100 $s^{1/2}$ (3 h) or less. It appears that for particles the size of the molding powder prills, the diffusion into or out of the HMX, binder, and prills all occurs on the same time scale. However, the lack of reproducibility of the *amount* of the rapid loss for the 95 → 42% experiment is evidence that HMX sorption is involved. The source of the long tail on two of the 95 → 42% experiments is unclear. It may involve the HMX and be due to the intermediate time (50–800 $s^{1/2}$) process seen in Figures 6 and 7, or it may simply be the outgassing of solvents (such as MEK and isopropyl alcohol) that were used in the production and storage of the PBX 9501. These experiments were performed with PBX 9501 that had not been baked out in a vacuum. Baking out *in vacuo* was begun in mid 2001, and samples run after that time show smaller long time tails.

Pressed and machined PBX 9501 cylinders

The PX experiments with machined cylinders in Figure 9 show Fickian behavior. We believe that this

is because all that is observed is absorption by the binder. The low RH experiments in Figure 10 on both machined and pressed cylinders of PBX 9501 performed at LANL show the same behavior, and the D coefficients obtained from the LANL and PX experiments are in good agreement. These effective diffusion coefficients are an order of magnitude smaller than the D in binder alone, but this is to be expected because the water in the thin layer of binder that coats the surfaces of the HMX particles must diffuse around the HMX particles, and the tortuosity and porosity of the material lower the effective D.[20] We note that, as is always the case with Fickian diffusion, the times required for gain and loss of water are the same.

On the other hand, the rapid, non-Fickian loss seen in the experiments in Figure 10 that start at high RH is clearly due to the HMX. Evidence of this same kind ($t^{1/2} \sim 50$ $s^{1/2}$ or 45 min) of rapid loss is also seen in Figures 6 through 8. However, no correspondingly rapid gain is seen in Figure 9, 10 or in any of our experiments. It appears that the sorption of water by the HMX in PBX 9501 must take much longer. In the tensile (''dog-bone'') samples, the sorption that can be attributed to the HMX did not begin to show until after about 45 days ($t^{1/2} \sim 2000$ $s^{1/2}$). The half inch cylinders of PBX 9501 that clearly showed the rapid loss due to the HMX had always spent correspondingly long times at high RH before the loss experiments began. The quantity of water sorbed by the HMX varied widely as already noted. However, this depended not only on how long the sample had been at the high RH but also on how many times it had been cycled between low and high relative humidities and probably also on the uncertainty in the high RH measurement.

We note that most of the LANL experiments that involved high RH were loss experiments because it was difficult to stabilize the balance chamber at high RH. However, to verify the ideas in the preceding paragraph, one experiment was performed in which the balance was held at 94% RH and the half inch machined cylinders of PBX 9501 were kept for some time at 0% RH and then transferred to the balance to see if there was any rapid gain. The results, shown as the top curve in Figure 10 show Fickian behavior with the same D as those of the high RH PX experiment shown in Figure 9. There was no rapid gain, and, for the 34 days for which the experiment could be run stably, there was also little or no slow weight gain that could be attributed to the HMX in the PBX 9501.

Also, to see if any of the rapid or ''extra'' mass lost in the experiments that involved HMX that started at high RH could be some solvent impurity that was displaced by the water at high RH, an experiment was done in which a sample of powdered HMX was left on the pan of the balance, and the RH in the balance chamber was cycled between 95 and 25% by changing the solutions used to control the RH in the balance chamber. The solutions were changed every 26 days, and the experiment ran through two and a half cycles (about 5 months). The balance chamber was opened and ventilated each time the solutions were changed, so that, if the loss involved solvent impurities, this experiment should have shown irreversible losses in mass. No net loss in mass was observed. Hence, all evidence indicates that all the rapid loss of mass is water.

The sorption behavior of the HMX, both neat and in PBX 9501, is so drastically non-Fickian that it must be considered to be adsorption, not absorption. We believe that, as already noted, it is condensation of water in pores or surface imperfections of the HMX crystals. Because water is more strongly attracted to the hydrophilic binder than to the hydrophobic HMX, it appears that in uptake experiments, the water goes into the binder first and then into or onto the HMX crystals. In loss experiments, it appears that the water is lost first from the HMX and then from the binder. However, the great difference in the time scales for the gain and loss of water from the HMX is intriguing. We do not yet see a clear answer to the following question: How does water then escape rapidly if it is in a pore on an HMX particle that is in the interior of a cylinder of PBX 9501? Comparing the two highest points in the upper right hand corner of Figure 3 (PBX cylinders) with the highest points in Figure 2 (HMX powder), we conclude that, in the high points in Figure 3, virtually all the HMX in this cylinder of PBX 9501 was participating in the uptake of water. Then, all this extra water left the cylinder in 150 $s^{1/2}$ (6 h) in the experiment shown as the lowest line in Figure 10. The only way we can see for this to happen is for the water that is adsorbed by the HMX to form pores along one HMX particle to the next all the way through the PBX. Then, it can rapidly escape back through those pores when the RH is suddenly lowered. Some reconstruction of pathways could be the cause of the early time moderately fast loss seen in the lowest curve in Figure 10. Furthermore, we believe that those pores must be filled back in by the binder reforming its hydrogen bonds with the HMX as the water adsorbed on the HMX leaves. Otherwise, the water in the binder would rapidly leave the PBX by the same route. It would only have to diffuse over a path on the order of a micron in length to get to a pore and then escape rapidly; on the contrary, it is clear from the longer time behavior in Figure 10 that the water absorbed by the binder diffuses all the way out of the cylinder by following

a path inside the binder. Thus, it appears that, at high RH, pores are formed that connect all the way through the solid PBX. In this state the density of pore sites is above the percolation threshold,[21] and water can move through them quite rapidly. However, when the RH is lowered, and the water on the HMX leaves rapidly, the pores get filled in by the binder, the density of pore sites drops below the percolation threshold,[21] and movement of the water becomes so much slower that it is dominated by diffusion through the binder. This is admittedly quite a tentative explanation, but we know of no other that is consistent with the experimental data.

CONCLUSIONS

In this article we have reported measurements of the sorption and loss of water by the components of PBX 9501. Both the quantities and the time dependences of the water gained and lost have been measured. Where possible, those processes have also been modeled and equilibrium constants and diffusion coefficients obtained.

The Estane[4] and binder display expected behavior with type III absorption isotherms and Fickian diffusion. The NP displays an ordinary type III absorption isotherm but somewhat non-Fickian diffusion-probably due to boundary layer formation on the surface of the liquid.

The neat HMX displays an extreme type III sorption isotherm characteristic of hydrophobic interactions; it sorbs very little water at low and moderate relative humidities but much more water at very high relative humidities. Its time dependence is not at all Fickian. We conclude that, except for small amounts of water that may be absorbed into a little γ-phase HMX that may be present, the dominant β-phase HMX present in our samples does not absorb water but has a hydrophobic interaction with water and only adsorbs it at such high relative humidities that the water is condensing into pores or surface imperfections of the HMX crystals.

The sorption of water by PBX 9501 is a composite of the behaviors of the binder and the HMX. At low relative humidities near linear absorption and Fickian diffusion are observed, and this is due to the binder phase. At high relative humidities sorption by the HMX phase is observed. This water is only slowly taken up, and it takes a long time for it to reach equilibrium. However, this same water is lost very rapidly when the RH is lowered even when the PBX has been pressed and machined into half inch cylinders. We believe that this behavior may involve some restructuring in the way the binder bonds to the surfaces of the small HMX crystals.

Results are given in Table II that allow the reader to estimate how long it will take to dry any of the components of PBX 9501.

We thank Gregg K. Sullivan and Jose G. Archuleta for sending us results prior to publication and Richard V. Browning for assistance and encouragement. We also thank Antonio Redondo for helpful suggestions. The work at Los Alamos National Laboratory was performed under the auspices of the National Nuclear Security Administration of the U. S. Department of Energy under Contract No. DE-AC52-06NA25396.

References

1. Benzinger, T. M. X-0242: A high energy plastic bonded explosive, LA-4872-MS; Los Alamos National Laboratory Report: Loa Alamos, NM, 1972.
2. Schollenberger, C. S. (to B. F. Goodrich Co.). U.S. Pat. 2,871,218 (1959).
3. Finger, M. Properties of BDNPA and BDNPF, eutectic mixture, Report UCID-16088; Lawrence Livermore National Laboratory: Livermore, CA, 1972.
4. Salazar, M. R.; Thompson, S. L.; Laintz, K. E.; Pack, R. T. J Polym Sci Part B: Polym Phys 2002, 40, 181.
5. Salazar, M. R.; Pack, R. T. J Polym Sci Part B: Polym Phys 2002, 40, 192.
6. Salazar, M. R.; Lightfoot, J. M.; Russell, B. G.; Rodin, W. A.; McCarty, M.; Wrobleski, D. A.; Orler, E. B.; Spieker, D. A.; Assink, R. A.; Pack, R. T. J Polym Sci Part A: Polym Chem 2003, 41, 1136.
7. Shipp, K. G.; Hill, M. E. J Org Chem 1966, 31, 853.
8. Castorina, T. C.; Haberman, J. Explosivstoffe 1969, 17, 176.
9. Castorina, T. C.; Haberman, J. The water adsorption properties of the polymorphs of HMX: The thermodynamics of water interaction with ground and unground β-HMX, Picatinny Arsenal Technical Report 3555; Picatinny Arsenal: New Jersey, 1967.
10. Mang, J. T.; Skidmore, C. B.; Hjelm, R. P.; Howe, P. M. J Mater Res 2000, 15, 1199.
11. Sullivan, G. K. PBX particle size distribution using an image analysis technique, LA-UR-00-5257; Los Alamos National Laboratory Report: Los Alamos, NM, 2000.
12. Sullivan, G. K. PBX particle size distribution using an image analysis technique, LA-UR-02-5078; Los Alamos National Laboratory Report: Los Alamos, NM, 2002.
13. Archuleta, J. G. DX-2, LANL, private communication, March 2003.
14. Gregg, S. J.; Sing, K. S. W. Adsorption, Surface Area and Porosity; Academic Press: New York, 1967; Chapter 3.
15. Crank, J. The Mathematics of Diffusion; Clarendon Press: Oxford, 1956; Chapter 1.
16. Neogi, P. In Diffusion in Polymers; Neogi, P., Ed.; Marcel Dekker: New York, 1996; p 173.
17. Smith, G. S.; Skidmore, C. B.; Howe, P. M.; Majewski, J. J Polym Sci Part B: Polym Phys 2004, 42, 3258.
18. Main, P.; Cobbledick, R. E.; Small, R. W. H. Acta Crystallogr Sect C 1985, 41, 1351.
19. Herrmann, M.; Engel, W.; Eisenreich, N. Z Kristallogr 1993, 204, 121.
20. Grathwohl, P. Diffusion in Natural Porous Media; Kluwer: Boston, 1998; pp 29–34.
21. Stauffer, D. Introduction to Percolation Theory; Taylor & Francis: London, 1985; pp 1–15.